Electric Control of Wetting by Salty Nanodrops: Molecular Dynamics Simulations

ARTICLE *in* THE JOURNAL OF PHYSICAL CHEMISTRY C · NOVEMBER 2011

Impact Factor: 4.77 · DOI: 10.1021/jp206242n

3 AUTHORS, INCLUDING:

Christopher David Daub

Norwegian University of Science and Techno…

29 PUBLICATIONS **417** CITATIONS

SEE PROFILE

THE JOURNAL OF PHYSICAL CHEMISTRY C

ARTICLE

pubs.acs.org/JPCC

Electric Control of Wetting by Salty Nanodrops: Molecular Dynamics Simulations

Christopher D. Daub, Dusan Bratko,* and Alenka Luzar*

Department of Chemistry, Virginia Commonwealth University, Richmond, Virginia 23284, United States

ABSTRACT: Aqueous nanoscale systems feature a distinct electrowetting behavior, sensitive to not only the strength but also the direction and polarity of the applied electric field. These effects have so far not been tested in solutions of ions, although electrolytes are commonly present in electrowetting experiments. We describe atomistic simulations of sessile salty nanodrops on an apolar substrate under electric fields in a miniature mimic of the experimental setup of a drop inside a capacitor. In the absence of field, the contact angle rises with salt concentration. The effect is weaker when the surface is more hydrophobic. The electric field lowers the contact angle, but the polarity dependence, observed in neat water and related to directional hydrogen bond effects, is diminished in the presence of screening ions. This is important for nanofluidics, as the addition of salt can improve electrowetting inside a nanopore where uneven wettabilities of opposing walls are found in pure water. The different hydration properties of cation and anion are reflected in their density profiles. The droplet curvature enhances ion withdrawal from the liquid/vapor interface, the depletion being more pronounced for cations (Na^+, Mg^{2+}) than anions (Cl^-). The dependence of the contact angle on the field strength varies nonmonotonically with salt concentration, suggesting that moderate concentrations represent the optimal regime for the electric control of wetting properties at the nanoscale.

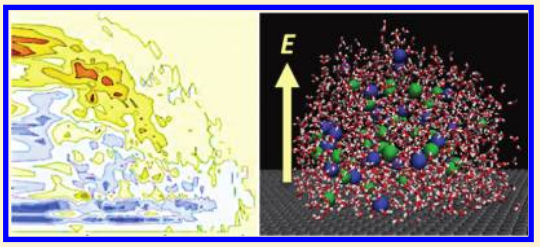

1. INTRODUCTION

The study of sessile liquid drops is a subject with a rich history, dating back to Young's equation which relates the contact angle θ_c of a macroscopic drop to the interfacial energies of each of the three components in the system

$$\cos\theta_c = (\gamma_{sv} - \gamma_{sl})/\gamma_{lv} \quad (1)$$

where $\gamma_{\alpha\beta}$ are the interfacial free energies of the three phases, solid (s), liquid (l), and vapor (v). If the drop is small, the line tension τ[1] also plays a role, $\cos\theta_c(r_B) = \cos\theta_c(\infty) - \tau/\gamma_{lv}r_B$, where $\theta_c(r_B)$ is the contact angle of a droplet with the base radius r_B[2] and $\theta_c(\infty)$ is the macroscopic (Young) contact angle (θ_c in eq 1).

Contact angles of model nanodrops have been within the reach of molecular simulations for quite some time now,[3] and over the years techniques to estimate contact angles and other relevant quantities have been refined.[4−6] In our previous work, we have examined sessile drops of neat water under the influence of electric fields,[7] as well as the influences of surface corrugation[8] and chemical heterogeneity[9] on the contact angle and transport properties of a nanodrop. In parallel studies, we deduced contact angle changes under an applied field from interfacial free energy calculations for aqueous films in narrow planar confinements.[10,11] These works revealed novel nanoscale electrowetting effects, absent in macroscopic experiments. Specifically, we have shown that the reduction in surface free energy, or equivalently in $\cos\theta_c$, depends on both the field direction and polarity.[7,10] Due to the generic preference of all dipolar molecules to polarize parallel to the interface,[12,13] and the angular bias of surface water molecules optimizing hydrogen bonding,[14,15] orientational polarization of interfacial water is strongest when the field is parallel to the interface. In electric field normal to the surface, polarization and concomitant reduction in contact angle are stronger when the field points into the aqueous phase. This polarity effect is of different origin and opposite to the known hydration preference of water to bind more tightly to an anion than a cation if size and van der Waals attraction to water are equal for both ions.[16−18]

It is clearly of interest to examine how nanoscale effects on electrowetting play out in the presence of salt ions, themselves strongly orienting adjacent water molecules. In this article, we present our findings on sessile nanodrops made up of water and dissolved salt (NaCl and $MgCl_2$), with and without the added presence of an electric field. In field-free systems, our calculations should shed light on the observed salt-induced increase in water/substrate interfacial tension,[19] traditionally attributed to image-charge ion/substrate repulsion.[20] As modulated interfacial tension impacts the forces among solute surfaces, our calculation complements existing molecular studies of the influence of salinity on the strength and range of hydrophobic interaction.[21−26] In the field, addition of salt ions should increase field screening, reducing the effective field strength in the interior of the droplet. In addition, relative attraction of different ions to the interface[27] could affect the interfacial properties and contribute to the sign asymmetry (polarity dependence) of the influence of the field. Our findings about salt effects in the absence of field complement scarce

Received: July 1, 2011
Revised: October 5, 2011
Published: October 10, 2011

experimental data[19,28] in showing a stronger increase in contact angles at hydrophilic surfaces. Experiments for hydrophobic substrates are inconclusive, showing weak changes of either sign, while our molecular simulations confirm a moderate increase in both the contact angle and wetting free energy of a hydrophobic surface upon addition of salt.

2. SIMULATION APPROACH

Model. We determine the microscopic analogue of the contact angle[3,4] of sessile nanodroplets with around 2000 molecules of the extended simple point charge model of water (SPC/E)[29] on a prototypical graphite-like lattice. The system can be exposed to a uniform external field, mimicking the experimental setup of Bateni et al.[30,31] where the drop is placed between insulated capacitor plates. The Lennard-Jones interactions between substrate atoms and water are tuned to mimic nonpolarizable surfaces with desired hydrophilicities using parametrization of Werder et al.[6] and do not attempt to emulate true graphite surfaces, characterized by strong induced-multipole attraction of ions.[32] The nanodroplets contain pure water, NaCl, or $MgCl_2$ solutions. We introduce salt at a given concentration by replacing the required number of water molecules with ions. We study NaCl solutions at concentrations of 1 M (1 M = 1 mol dm^{-3}) with 1928 H_2O molecules, 36 Na^+, and 36 Cl^- ions and 4 M (1712 H_2O, 144 Na^+, and 144 Cl^-) and a $MgCl_2$ solution at a concentration of 1 M (1894 H_2O, 36 Mg^{2+}, and 72 Cl^-). The potential models for the ions taken from Koneshan et al.[33] and Aqvist[34] are well suited to solutions with SPC/E water. The usual combining rules are used to determine interactions between unlike ions and between ions and water.

Molecular Dynamics Simulations. Computer simulations are carried out with the LAMMPS molecular dynamics code[35] in the NVT ensemble. The temperature (300 K) is maintained by a Nosé-Hoover thermostat[36] with 0.1 ps time constant, and the simulation time step is 1 fs with Verlet integrator. Lennard-Jones interactions are truncated smoothly at 14.0 Å. Nontruncated electrostatic interactions are treated by the particle−particle particle mesh solver (pppm)[37] with a real space cutoff of 11.0 Å and precision tolerance of 10^{-5}. For situations of our present interest, this seemed to greatly reduce the importance of finite-size effects or, equivalently, the magnitude of the line tension, compared to previous simulations where a cutoff was applied to Coulombic interactions.[6,7] In view of the droplet's coexistence with its own vapor, pressure remains close to the vapor pressure of water throughout the simulation. Extra height (300 Å) of the simulation box minimizes interactions with the system's periodic images in the z direction.

Water Contact Angle Calculations. To measure the microscopic analogue of the macroscopic contact angles on the surface, we use the drop analysis technique developed by de Ruijter et al.,[5] where contact angles are computed from circular drop contours extrapolated to the substrate surface as described in detail in refs 6 and 7. Each system is equilibrated for at least 500 ps and typically runs for an additional 5 ns to secure contact angle convergence. For very hydrophilic surfaces, production runs of up to 10 ns were made. We record the trajectories with a 1 ps interval. In each recorded configuration, cylindrical binning was used to get the water drop isochores. The surface normal passing through the center of mass of the droplet is used as the reference axis. The bin height is 0.5 Å, and the base area per bin is 50 $Å^2$, so that all bins are of equal volume. From the profile, the equimolar dividing surface is determined in each horizontal layer of the binned drop, and a circular fit through these points is extrapolated to the reference plane to measure the contact angle.

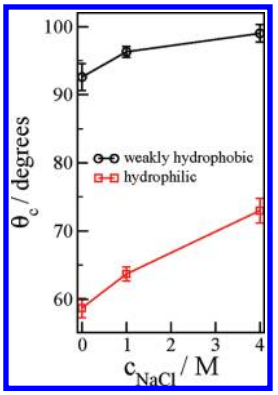

Figure 1. Contact angles as a function of the concentration of NaCl on surfaces with different Lennard-Jones well depth, determined from several 400 ps MD simulations. Error bars are one standard deviation in the mean.

As pointed out in ref 5, the circular contour becomes distorted below a certain height related to the range of wall−liquid molecular correlation. Above this height, the contour curvature is constant and can be used in contact angle calculation. A further increase in the cutoff has no effect on the result. The empirical cutoff height (satisfying convergence) we used was typically two or three water diameters above the substrate.

We have not noticed any systematic variation in the contact angle with larger aqueous drops with 4000 and 8000 molecules.[38] In previous work, we also compared the contact angle of the nanodroplet with the result obtained by calculating the wetting free energy from thermodynamic integration[9] and water surface tension obtained by the pressure tensor method.[10] The Young contact angle, eq 1, matched the result obtained from the nanodroplet geometry within simulation uncertainties of 3°. These results suggest line tension should not exceed 2×10^{-11} N, which is somewhat below the value of 7×10^{-11} N measured for micrometer droplets[39,40] but well within theoretical expectations[41,42] and close to estimates from computational line tension studies comparing truncated-sphere nanodroplets and zero perimeter curvature drops of cylindrical geometry.[43]

3. RESULTS

3.1. Effect of NaCl Concentration on Contact Angles. In Figure 1 we show contact angles in NaCl solutions in the absence of an external field. Contact angles are measured as a function of concentration for prototypical graphite-like surfaces with two different Lennard-Jones well depths, ε_{CC} = 0.387 and 0.205 kJ/mol, which lead to surfaces with two different hydrophilicities. The contact distance σ = 3.214 Å was used in both cases. In pure water, these surfaces are characterized by contact angles of 58.5 or 92.5°. The contact angle is considerably increased by the addition of salt. Equation 1 can provide an estimate of surface wetting free energy $\gamma_{sl} - \gamma_{sv}$ from calculated contact angles and known surface tensions of salt solutions.[19] According to contact angle changes shown in Figure 1, the addition of 4 M NaCl raises the wetting free energy of the simulated hydrophilic surface from −38 to −23 mN/m and from 2.5 to 11 mN/m for the weakly hydrophobic one. While these values represent only rough estimates,

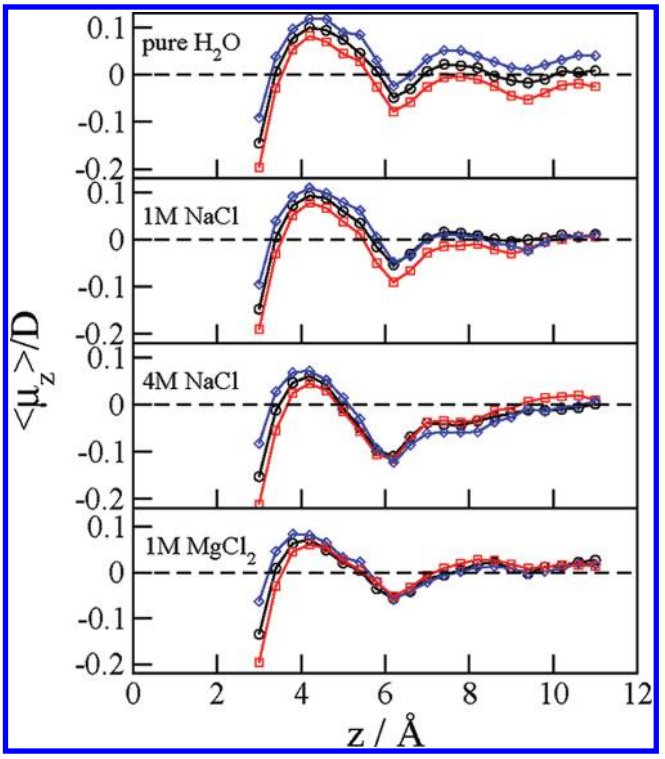

Figure 2. Component of the water dipole (in Debye units) perpendicular to the solid surface as a function of the height above the surface z. Black lines are without field. Blue and red lines are, respectively, in a positive and negative external field of strength 0.045 V/Å. Error bars are approximately ±0.004 D for pure water throughout the plotted range of z. For the ionic solutions, the error bars are the same at small z but rise to approximately ±0.01 D for the 1 M systems and ±0.015 D for the 4 M system.

the changes in wetting free energies conform to salting-out effects of moderately soluble particles.[21,23−25] The greater disparity in contact angle increases is due to the increase of the solution/vapor surface tension. This change shifts the contact angle closer to 90°, raising it further at hydrophilic surfaces and reducing it on the hydrophobic ones. Both the increase in contact angles and the comparatively greater sensitivity to salt in the case of hydrophilic surfaces are in agreement with experimental data of refs 19 and 28. Recent measurements and model calculations on molecularly heterogeneous TiO_2/OTHS surfaces reveal a weak decline in contact angle upon addition of salt.[44] Ion adsorption associated with the presence of strongly polar TiO_2 patches can explain this reduction, absent on more uniform, apolar, or moderately polar surfaces.[19,28] Our model surface, which owes its affinity for water to enhanced dispersion forces, cannot capture the ion adsorption such as that observed on muscovite surfaces[45,46] and expected on exposed TiO_2 sites.

3.2. Structure of Salt Water Droplets under Electric Field.

All calculations in the presence of electric field were carried out on the moderately hydrophobic surface (zero-field water contact angle 92.5°). Figure 2 shows the plots of the component of the water dipole perpendicular to the surface in fields of positive and negative polarity as a function of height z, i.e., vertical distance from the surface. Only the central section of the droplet's base of radius 2 nm is considered in these calculations to remove any effects of the drop fluctuations at the perimeter. Results for pure water, 1 and 4 M NaCl, and 1 M $MgCl_2$ are shown. The strength of the uniform external field before reduction due to dielectric screening is 0.045 V/Å. The dielectrically shielded field inside the salt-free drop, deduced from observed polarization by the field,[47] is about 20 times weaker and position dependent. The addition of salt results in further shielding of the field. When no field is applied, water molecules in the layer closest to the solid interface take on an average orientation mildly skewed toward pointing out of the drop into the interface.[14,15] Depending on polarity, the external field acts to either enhance or reduce this orientation. Even in the strong applied field we used, spontaneous orientation of interfacial molecules is much more prominent than the field-alignment effect. In pure water, a damped layering is observed not only in water density but also in the dipole orientation, which is further modulated by the effective electric field at different locations in the water drop.

In the absence of ions, the effect of the electric field on the water dipoles' orientation is approximately constant throughout the drop. This means that, with the exception of a thin surface layer, dielectric screening is approximately uniform inside the drop, similar to observed behavior in slab geometry.[48] The situation is markedly different in the salty water drop. Since there remains a layer of water separating ions from the solid surface at all concentrations, the water molecules nearest the surface behave as they do in pure water drops. However, the effect of ion screening comes into play further inside the drop. At the lower concentration of 1 M, at a distance z > 10 Å, the ions have screened the field to such an extent that there is no longer any discernible effect on the dipolar orientation. Even more interesting is the effect of ion screening, observed beyond the first monolayer of water and counterions at the high ionic strengths in 4 M NaCl and 1 M $MgCl_2$ solutions. Here we can see that at distances z > 7 Å the high concentration of ions has caused an overcompensation of the water dipole orientation, such that the water dipoles are affected by the electric field in the opposite way than one would expect. A similar counterintuitive result has been observed in other systems, where overcompensation was associated with combined ion-dipole shielding[49−51] or pure ionic effects.[52−54]

An important consideration in understanding the salt water droplets is the degree of ion adsorption to the surface. In Figure 3, we show the structure of the 4 M NaCl solution as a function of the height above the surface. The oscillatory structure of water

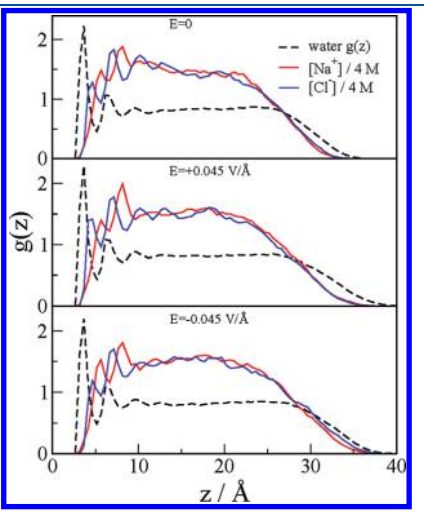

Figure 3. Plot of $g(z)$ of water molecules and ions as functions of height above the surface z. $g(z)$ is the ratio of local and average concentrations of a given species in the drop (4 M NaCl).

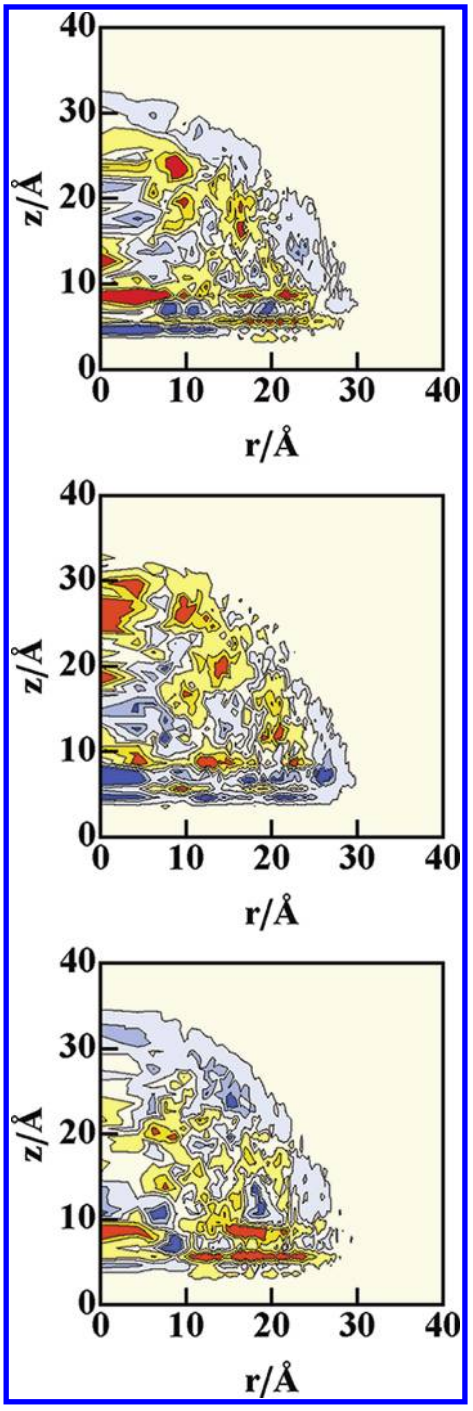

Figure 4. Charge density plots of 1 M NaCl sessile nanodrops in the absence of electric field (top) and in a field of +0.045 V/Å (middle) and −0.045 V/Å (bottom). The total run length in each case was 4 ns. The color scheme runs from $0.001e_0$ Å^{-3} (dark orange) to $-0.001e_0$ Å^{-3} (dark blue).

strongly resembles the density distribution of hydration water deduced from X-ray reflectivity at the mica (001)/water interface.[55] The single density peak in the first hydration shell reflects the absence of solid/water hydrogen bonding, as opposed to the double peak observed on mica due to a slight distinction between adsorbed (hydrogen bonded) and nonbonded hydration water on mica.[45,46,55] On the nonpolar model surface, we see that the anions are closer to the surface than the cations; however, there is essentially no ion adsorption. There always remains a layer of water between the first ionic layers and the surface, and co-ion depletion contributes importantly to the double layer formation. Furthermore, the ion concentrations in the middle of the drop (close to 6 M) are considerably greater than the average concentration of 4 M, reflecting the ions' avoidance of the surface. The comparatively greater affinity of the anion (Cl^-) than cation (Na^+) for both the solid/liquid and liquid/vapor interfaces agrees with observations from other groups.[56−58] Analogous trends are seen in the $MgCl_2$ solution (not shown). The effect of the electric field agrees with expectations. The introduction of polarizable ion force fields could somewhat influence the ion distribution since polarizable models are already known to favor surface exposure at the liquid−vapor interface.[59,60] These effects are, however, very weak for Na^+ and Mg^{2+} ions, and Cl^- represents a border case[25,60] with only slightly enhanced surface concentration due to ion polarizability.[61,62] Despite the shallow minimum in the potential of mean force of the Cl^- ion right next to the surface, the *overall* interfacial depletion associated with the measured surface tension of NaCl solutions is essentially the same as in the case of NaF.[63] If using a polarizable model for water, ion−ion interactions[64] and ion distribution at vapor[65] and solid[26] interfaces could also be somewhat affected by water polarization in the local fields of the ions. The externally applied electric fields we use are, however, at least an order of magnitude too weak to cause any detectable polarization of the ions of water molecules (see also discussion in Section 3.3).

Figure 4 shows the charge density of the 1 M NaCl nanodrops, in the absence of field and in fields of ±0.045 V/Å. We see that in the absence of electric field the Cl^- ions have a greater affinity for the interfaces than the Na^+ ions, which are more prevalent within the second layer (Figure 3 top, Figure 4 top). This agrees with the commonly accepted picture of ions at interfaces acquired in classical molecular simulations and further enhanced in more elaborate, polarizable models.[59−61,63,66−69] The difference in both size and polarizability contributes to the relative preference of Cl^- ions to reside closer to the interface, and this trend is captured by properly optimized nonpolarizable force fields.[68] Interestingly, our results shown in Figure 3 top and Figure 4 top suggest that curvature *enhances* ion depletion at the convex surface where the loss of favorable hydration is more pronounced. In the droplet, both species are depleted from the interface, but more so for Na^+ ions, resulting in net negative surface charge density. In fact, even a large electric field pointing toward the surface, which should increase the affinity of positive ions for the surface, is not sufficient to completely overcome the negatively charged layer near the model graphite surface. Larger fields which could bring ions to the outer surfaces of the drop would also cause those ions to be desorbed from the drop, with the first hydration shell staying with the ion (see below).

Observed structural changes suggest two opposing effects of added salt on nanodrop electrowetting. The energetically favorable formation of an electric double layer enhances electrowetting and reduces contact angle.[44,70,71] Ionic screening, however, weakens the influence of the field inside the droplet core. The competition between these effects suggests the possibility of nonmonotonic dependence on salt concentration, and this appears consistent with our results presented in the following section.

3.3. Effect of Electric Field on Contact Angles. The contact angle of aqueous nanodrops at different salt concentrations is shown as a function of electric field strength and direction in

Figure 5. Note that the nonscreened fields, listed as the input to the simulation, exceed by over an order of magnitude the average field across the droplet after the dielectric screening is taken into

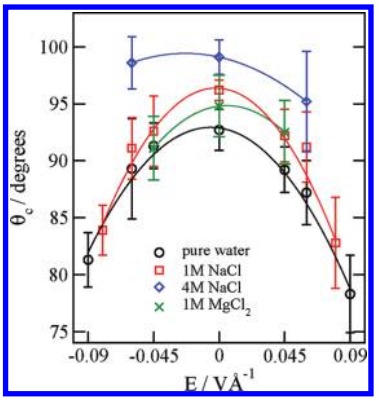

Figure 5. Contact angles as a function of electric field strength of pure water, NaCl solutions of differing concentrations, and $MgCl_2$ on a model apolar surface, determined from several 400 ps MD simulations. Error bars are one standard deviation in the mean.

account. With this in mind, the actual field strengths spanning our simulated droplets remain below the fields inside ion channels,[72] next to polyelectrolytes,[73,74] at an AFM tip and in a micron-scale capacitor.[75] Fields of comparable strength are known to reduce the interfacial free energy of aqueous interfaces with another liquid,[76] solid,[7,10] or vapor.[10] For the salt water drops, contact angles decrease in the presence of the electric field, and within the simulation uncertainty, the amount of the decrease is the same regardless of field polarity. The shape of the curve $\cos\theta_c(E)$ resembles experimental dependences of θ_c in electrowetting experiments in ionic liquids,[77,78] as well as in titration curves where the external field is replaced by varied charge density of an ionized substrate.[44] The overall decrease agrees with our previous work.[7] However, in pure water we observe a noticeable asymmetry in contact angle response to the field[7] in agreement with studies in slit geometry.[10,11,79,80] This asymmetry is suppressed when salt solutions are considered. We attribute this difference to the increased screening of the electric field by the Na^+, Mg^{2+}, and Cl^- ions, the asymmetry in the strength of cation and anion hydration, and their affinities toward the substrate that can all blur the subtle differences in hydrogen bonding which produce the asymmetry in the case of pure water nanodrops.

3.4. Field-Induced Ion Evaporation. At fields somewhat larger than those applied above, it is possible to observe the evaporation of hydrated ions from the droplet, in a phenomenon closely related to ion desorbtion in electrospray ionization mass spectroscopy. In our simulations, we have noticed that a field perpendicular to the surface of magnitude >0.08 V/Å is sufficient to cause the ions to escape the top surface of the drop. This field strength is in line with other estimates from electrospray experiments[81] and simulations.[82] If the field is applied parallel to the surface, ions accompanied by surrounding water molecules will sporadically leave the droplet at even lower field strengths (≈0.05 V/Å). The relative ease of desorption in these cases is explained in terms of weaker dielectric screening of the parallel field[10,12] and the ability of the runaway ion/water cluster to glide along the solid surface, thus retaining the favorable interaction with the substrate.

4. DISCUSSION

Orientational polarization of water in a sessile nanodroplet exposed to external field is most pronounced at droplet interfaces, lowering interfacial free energy and contact angle. For experimentally realizable strengths of applied field, molecular alignment with the field remains weak in comparison to spontaneous polarization of surface molecules oriented to optimize hydrogen bonding. In pure water, the coupling of spontaneous polarization and alignment with the field results in polarity dependence of nanoelectrowetting.[7,10,11,80,83] When salt is dissolved in the drop, contact angles continue to decrease in the presence of electric field. At the lower concentration of 1 M, the amount of the decrease is the same regardless of field polarity. On the whole, the contact angle decrease due to the field in 1 M NaCl is somewhat bigger than in pure water, in qualitative agreement with experiments in diluted salt solutions.[44] The lack of polarity dependence of the contact angles seen in pure water drops is attributed to the screening of the electric field by Na^+ and Cl^- ions, which interferes with the differences in hydrogen bonding of interfacial water molecules at opposite orientations. Addition of a moderately concentrated salt can therefore improve the field-induced wetting inside a nanopore where strong asymmetry in wettabilities of opposing surfaces is observed[10,11,80] in pure water. An asymmetric dependence of a different origin can be anticipated from the microscopic structure of the electric double layers formed next to the solid upon imposition of the field (Figures 3 and 4). Asymmetric electrowetting associated with different cation and anion affinities to the substrate has been detected in experiments[77,84] and is indicated by contact angles we observe at the higher salt concentration of 4 M, although the error bars are too big for a firm conclusion.

In agreement with measurements on nonpolar or moderately polar substrates,[19,28] the contact angle in our model system rises upon addition of salt. The effect of salt on the field-induced reduction in contact angle, however, appears nonmonotonic, enhancing the field effect at 1 M concentration, but not at 4 M. A likely explanation invokes interplay of two opposing effects suggested by salt and water structures shown in Figures 2−4. First, according to the Gibbs adsorption isotherm, the redistribution of ions, which respond to the imposition of the field by forming a double layer next to the substrate surface, reduces the solid/solution interfacial tension γ_{sl} and therefore the contact angle.[44,71] The increase in surface concentration of ions, and concomitant contact angle reduction, is limited by the strength of the external field and cannot be enhanced further by increasing salt concentration. Second, the ordering of water dipoles around the ions will interfere with the orientational polarization by the external electric field. This weakens the influence of the field on the contact angle, and the weakening intensifies with salt concentration.

It is well-known that the smaller Na^+ cation binds its hydration water more tightly than the Cl^- anion.[85] Because of screening effects, the electric field in the droplet is most prominent in a thin layer adjacent to the substrate. High salt concentrations and negative field E ($d\psi/dz > 0$, where ψ is electrostatic potential) lead to the increased presence of Na^+ ions near the solid surface, which should weaken electrowetting in 4 M NaCl. Conversely, in the positive field the interface is enriched in Cl^- ions. The comparatively looser hydration of Cl^- can accommodate stronger orientational polarization of water by the applied field and hence stronger contact angle reduction at high concentration when the field is positive. While average contact angles in 4 M salt

conform to expectation from calculated structures, statistical uncertainties preclude a definitive validation of the above picture.

5. CONCLUSIONS

Dissolution of salt in an aqueous nanodroplet on a nonpolar substrate results in higher contact angle, which reflects a combined effect of increased solid/solution[19] and solution/vapor[86] surface free energies. The increase in the wetting free energy is stronger on hydrophilic than on hydrophobic surfaces. When the sessile droplet is placed in a strong electric field inside a capacitor, the contact angle decreases with the strength of the field. Polarity dependence, observed in electrowetting in neat water, is suppressed in the presence of salt. The asymmetry in $\theta_c(E)$ dependence between positive and negative fields indicated in a highly concentrated electrolyte can be attributed to unequal hydration properties of salt cations and anions, unlike the reported asymmetry in pure water, explained in terms of interfacial hydrogen bonding effects.[7] Both mechanisms are significant primarily at the nanoscale, where a statistically significant fraction of molecules reside at the interfaces.

While the drop-in-capacitor setup[31] modeled in the present work features comparatively low sensitivity of contact angle to the field, identical qualitative trends are expected to apply to open systems. There, the field effects are much stronger as water can be driven from the environment into field-exposed domains.[7,10,11,80,87] According to our present results, the dependences on the field strength and direction can vary nonmonotonically with salt concentration suggesting that moderate concentrations represent the most interesting regime for the electric control of wetting properties at the nanoscale.

AUTHOR INFORMATION

Corresponding Author

*E-mail: aluzar@vcu.edu, dbratko@vcu.edu

ACKNOWLEDGMENT

We gratefully acknowledge the support of the Office of Basic Energy Sciences, U.S. Department of Energy (DE-SC-0004406). This research used resources of the National Energy Research scientific Computing Center, which is supported by the Office of Science of the U.S. Department of Energy under Contract No. DE-AC02-05CH11231.

REFERENCES

(1) Wang, J. Y.; Betelu, S.; Law, B. M. *Phys. Rev. E* **2001**, *63*, 031601–1.
(2) Widom, B. *J. Phys. Chem.* **1995**, *99*, 2803–2806.
(3) Hautman, J.; Klein, M. L. *Phys. Rev. Lett.* **1991**, *67*, 1763–1766.
(4) Mar, W.; Hautman, J.; Klein, M. L. *Comput. Mater. Sci.* **1995**, *3*, 481–497.
(5) de Ruijter, M. J.; Blake, T. D.; Coninck, J. D. *Langmuir* **1999**, *15*, 7836–7847.
(6) Werder, T.; Walther, J. H.; Jaffe, R. L.; Halicioglu, T.; Koumoutsakos, P. *J. Phys. Chem. B* **2003**, *107*, 1345–1352.
(7) Daub, C. D.; Bratko, D.; Leung, K.; Luzar, A. *J. Phys. Chem. C* **2007**, *111*, 505–509.
(8) Daub, C. D.; Wang, J.; Kudesia, S.; Bratko, D.; Luzar, A. *Faraday Discuss.* **2010**, *146*, 67–77.
(9) Wang, J. H.; Bratko, D.; Luzar, A. *Proc. Natl. Acad. Sci. U.S.A.* **2011**, *108*, 6374–6379.
(10) Bratko, D.; Daub, C. D.; Leung, K.; Luzar, A. *J. Am. Chem. Soc.* **2007**, *129*, 2504–2510.
(11) Bratko, D.; Daub, C. D.; Luzar, A. *Faraday Discuss.* **2009**, *141*, 55–66.
(12) Klapp, S. H. L.; Schoen, M. *J. Chem. Phys.* **2002**, *117*, 8050–8062.
(13) Klapp, S. H. L.; Schoen, M. *J. Mol. Liq.* **2004**, *109*, 55–61.
(14) Luzar, A.; Svetina, S.; Zeks, B. *J. Chem. Phys.* **1985**, *82*, 5146–5154.
(15) Lee, C. Y.; McCammmon, J. A.; Rossky, P. J. *J. Chem. Phys.* **1984**, *80*, 4448–4455.
(16) Lynden-Bell, R. M.; Rasaiah, J. C. *J. Chem. Phys.* **1997**, *107*, 1981–1991.
(17) Dzubiella, J.; Hansen, J.-P. *J. Chem. Phys.* **2004**, *121*, 5514–5530.
(18) Rajamani, S.; Truskett, T. M.; Garde, S. *Proc. Natl. Acad. Sci. U.S.A.* **2005**, *102*, 9475–9480.
(19) Sghaier, N.; Prat, M.; Nasrallah, S. B. *Chem. Eng. J.* **2006**, *122*, 47–53.
(20) Bratko, D.; Jonsson, B.; Wennerstrom, H. *Chem. Phys. Lett.* **1986**, *128*, 449–454.
(21) Kalra, A.; Tugcu, N.; Cramer, S. M.; Garde, S. *J. Phys. Chem. B* **2001**, *105*, 6380–6386.
(22) Graziano, G. *Chem. Phys. Lett.* **2009**, *483*, 67–71.
(23) Graziano, G. *Chem. Phys. Lett.* **2010**, *491*, 54–58.
(24) Zangi, R.; Berne, B. J. *J. Phys. Chem. B* **2006**, *110*, 22736–22741.
(25) Zangi, R.; Hagen, M.; Berne, B. J. *J. Am. Chem. Soc.* **2007**, *129*, 4678–4686.
(26) Bauer, B. A.; Patel, S. *J. Phys. Chem. B* **2010**, *114*, 8107–8117.
(27) Tavares, F. W.; Bratko, D.; Blanch, H. W.; Prausnitz, J. M. *J. Phys. Chem. B* **2004**, *108*, 9228–9235.
(28) Cserhati, T.; Forgacs, E.; Oros, G. *J. Biochem. Biophys.* **1999**, *38*, 1–15.
(29) Berendsen, H. J. C.; Grigera, J. R.; Straatsma, T. P. *J. Phys. Chem.* **1987**, *91*, 6269–6271.
(30) Bateni, A.; Susnar, S. S.; Amirfazali, A.; Neumann, A. W. *Langmuir* **2004**, *20*, 7589–7597.
(31) Bateni, A.; Laughton, S.; Tavana, H.; Susnar, S. S.; Amirfazali, A.; Neumann, A. W. *J. Colloid Interface Sci.* **2005**, *283*, 215–222.
(32) Walther, J. H.; Werder, T.; Jaffe, R. L.; Gonnet, P.; Bergdorf, M.; Zimmerli, U.; Koumoutsakos, P. *Phys. Chem. Chem. Phys.* **2004**, *6*, 1988–1995.
(33) Koneshan, S.; Rasaiah, J. C.; Dang, L. X. *J. Chem. Phys.* **2001**, *114*, 7544–7555.
(34) Aqvist, J. *J. Phys. Chem.* **1990**, *94*, 8021–8024.
(35) Plimpton, S. J. *J. Comput. Phys.* **1995**, *117*, 1–19.
(36) Evans, D. J.; Holian, B. L. *J. Chem. Phys.* **1985**, *83*, 4069–4074.
(37) Darden, T.; York, D.; Pedersen, L. *J. Chem. Phys.* **1993**, *98*, 10089–10092.
(38) Daub, C. D. *Faraday Discuss., Gen. Discuss.* **2010**, *146*, 96.
(39) Pompe, T.; Herminghaus, S. *Phys. Rev. Lett.* **2000**, *85*, 1930–1933.
(40) Pompe, T.; Fery, A.; Herminghaus, S. *Contact Angle, Wettability and Adhesion*, 2nd International Symposium on Contact Angle, Wettability and Adhesion June 21−23, 2000 Newark, NJ MST Conf.; 2002; Vol. 2, pp 377−386
(41) Rowlinson, J. S.; Widom, B. *Molecular Theory of Capillarity*; Oxford University Press: Oxford, 1982.
(42) Churaev, N. V.; Starov, V. M.; Derjaguin, B. V. *J. Colloid Interface Sci.* **1982**, *89*, 16–24.
(43) Weijs, J. H.; Marchand, A.; Andreotti, B.; Lohse, D. *Phys. Fluids* **2011**, *23*, 022001.
(44) Hanly, G.; Fornasiero, D.; Ralston, J.; Sedev, R. *J. Phys. Chem. C* **2011**, *115*, 14914–14921.
(45) Sakuma, H. *Geochim. Cosmochim. Acta* **2011**, *75*, 5366–5366.
(46) Sakuma, H.; Kawamura, K. *Geochim. Cosmochim. Acta* **2011**, *75*, 63–81.
(47) Sutmann, G. *J. Electroanal. Chem.* **1998**, *450*, 289–302.
(48) Ballenegger, V.; Hansen, J. P. *J. Chem. Phys.* **2005**, *122*, 114711.

(49) Patra, C. N.; Gosh, S. K. *Phys. Rev. E* **1993**, *48*, 1154–1162.
(50) Boda, D.; Chan, K. Y.; Henderson, D. *J. Chem. Phys.* **1998**, *109*, 7362–7371.
(51) Kohlmeyer, A.; Hartnig, C.; Sohr, E. *J. Mol. Liq.* **1999**, *78*, 233–253.
(52) Wu, J. Z.; Bratko, D.; Prausnitz, J. M. *Proc. Natl. Acad. Sci. U.S.A.* **1998**, *95*, 15169–15172.
(53) Das, T.; Bratko, D.; Bhuiyan, L. B.; Outhwaite, C. W. *J. Chem. Phys.* **1997**, *107*, 9197–9207.
(54) Kalcher, J.; Schultz, J. C. F.; Dzubiella, J. *J. Chem. Phys.* **2010**, *133*, 184511.
(55) Cheng, L.; Fenter, P.; Nagy, K. L.; Schlegel, M. L.; Sturchio, N. C. *Phys. Rev. Lett.* **2001**, *87*, 156103.
(56) Criscenti, L. J.; Cygan, R. T.; Kooser, A. S.; Moffat, H. K. *Chem. Mater.* **2008**, *20*, 4682–4693.
(57) Argyris, D.; Ashby, P. D.; Striolo, A. *ACS Nano* **2011**, *5*, 2215–2223.
(58) Willard, A. P.; Reed, S. K.; Madden, P. A.; Chandler, D. *Faraday Discuss.* **2009**, *141*, 423–441.
(59) Dang, L. X.; Chang, T. M. *J. Phys. Chem. B* **2002**, *106*, 235–238.
(60) Caleman, C.; Hub, J. S.; van Maaren, P. J.; van der Spoel, D. *Proc. Natl. Acad. Sci. U.S.A.* **2011**, *108*, 6838–6842.
(61) Jungwirth, P.; Tobias, D. J. *Chem. Rev.* **2006**, *106*, 1259–1281.
(62) Petersen, P. B.; Saykally, R. J. *Annu. Rev. Phys. Chem.* **2006**, *57*, 333–364.
(63) Pegram, L. M.; Record, M.T. *J. Phys. Chem. B* **2007**, *111*, 5411–5417.
(64) Smith, D. E.; Dang, L. X. *J. Chem. Phys.* **1994**, *100*, 3757–3766.
(65) A.Bauer, B.; Patel, S. *J. Chem. Phys.* **2010**, *132*, 024713.
(66) Hummer, G.; Garde, S.; Garcia, A. E.; Pratt, L. R. *Chem. Phys.* **2000**, *258*, 349–370.
(67) Noah-Vanhoucke, J.; Geissler, P. L. *Proc. Natl. Acad. Sci. U.S.A.* **2009**, *106*, 15125–15130.
(68) Horinek, D.; Herz, A.; Vrbka, L.; Sedlmeier, F.; Mamatkulov, S. I.; Netz, R. R. *Chem. Phys. Lett.* **2009**, *479*, 173–183.
(69) Amotz, D. B. *Phys. Chem. Lett.* **2011**, *2*, 1216–1222.
(70) Onuki, A. *J. Chem. Phys.* **2008**, *128*, 224704.
(71) Monroe, C. W.; Daikhin, L. I.; Urbakh, M.; Kornyshev, A. A. *Phys. Rev. Lett.* **2006**, *97*, 136102.
(72) Dzubiella, J.; Allen, R. J.; Hansen, J. P. *J. Chem. Phys.* **2004**, *120*, 5001–5004.
(73) Bratko, D.; Dolar, D. *J. Chem. Phys.* **1984**, *80*, 5782.
(74) Wagner, K.; Keyes, E.; Kephart, T. W.; Edwards, G. *Biophys. J.* **1997**, *73*, 21–30.
(75) (a) Philippsen, A.; Im, W. P.; Engel, A.; Schirmer, T.; Roux, B.; Muller, D. J. *Biophys. J.* **2002**, *82*, 1667–1676. (b) Song, C.; Wang, P. *Rev. Sci. Instruments* **2010**, *81*, 054702.
(76) Schweighofer, K. J.; Benjamin, I. *J. Electroanal. Chem.* **1995**, *391*, 1–10.
(77) Paneru, M.; Priest, C.; Sedev, R.; Ralston, J. *J. Am. Chem. Soc.* **2010**, *132*, 8301–8308.
(78) Paneru, M.; Priest, C.; Sedev, R.; Ralston, J. *J. Phys. Chem. C* **2010**, *114*, 8383–8388.
(79) Vaitheeswaran, S.; Yin, H.; Rasaiah, J. C. *J. Phys. Chem. B* **2005**, *109*, 6629–6635.
(80) Daub, C. D.; Bratko, D.; Luzar, A. *Top. Curr. Chem.* **2011**, DOI: 10.1007/128_2011_188.
(81) Fenn, J. B.; Rosell, J.; Meng, C. K. *J. Am. Soc. Mass. Spectrom.* **1997**, *8*, 1147–1157.
(82) Luedtke, W. D.; Landman, U.; Chiu, Y.-H.; Levandier, D. J.; Dresler, R. A.; Sok, S.; Gordon, S. S. *J. Phys. Chem. A* **2008**, *112*, 9628–9649.
(83) Daub, C. D.; Bratko, D.; Ali, T.; Luzar, A. *Phys. Rev. Lett.* **2009**, *103*, 207801.
(84) Quinn, A.; Sedev, R.; Ralston, J. *J. Phys. Chem. B* **2003**, *107*, 1163–1169.
(85) Mancinelli, R.; Botti, A.; Bruni, F.; Ricci, M. A.; Soper, A. K. *J. Phys. Chem. B* **2007**, *111*, 13570–13577.
(86) Bhuiyan, L. B.; Bratko, D.; Outhwaite, C. W. *J. Phys. Chem.* **1991**, *95*, 336–340.
(87) Bratko, D.; Daub, C. D.; Luzar, A. *Phys. Chem. Chem. Phys.* **2008**, *10*, 6807–6813.